



HAL
open science

Agent-based simulation of Notch mediated tip cell selection in angiogenic sprout initialisation

Katie Bentley, Holger Gerhardt, Paul A. Bates

► **To cite this version:**

Katie Bentley, Holger Gerhardt, Paul A. Bates. Agent-based simulation of Notch mediated tip cell selection in angiogenic sprout initialisation. *Journal of Theoretical Biology*, 2009, 250 (1), pp.25. 10.1016/j.jtbi.2007.09.015 . hal-00554493

HAL Id: hal-00554493

<https://hal.science/hal-00554493>

Submitted on 11 Jan 2011

HAL is a multi-disciplinary open access archive for the deposit and dissemination of scientific research documents, whether they are published or not. The documents may come from teaching and research institutions in France or abroad, or from public or private research centers.

L'archive ouverte pluridisciplinaire **HAL**, est destinée au dépôt et à la diffusion de documents scientifiques de niveau recherche, publiés ou non, émanant des établissements d'enseignement et de recherche français ou étrangers, des laboratoires publics ou privés.

Author's Accepted Manuscript

Agent-based simulation of Notch mediated tip cell selection in angiogenic sprout initialisation

Katie Bentley, Holger Gerhardt, Paul A. Bates

PII: S0022-5193(07)00443-2
DOI: doi:10.1016/j.jtbi.2007.09.015
Reference: YJTBI 4852

To appear in: *Journal of Theoretical Biology*

Received date: 11 January 2007
Revised date: 11 September 2007
Accepted date: 12 September 2007

Cite this article as: Katie Bentley, Holger Gerhardt and Paul A. Bates, Agent-based simulation of Notch mediated tip cell selection in angiogenic sprout initialisation, *Journal of Theoretical Biology* (2007), doi:[10.1016/j.jtbi.2007.09.015](https://doi.org/10.1016/j.jtbi.2007.09.015)

This is a PDF file of an unedited manuscript that has been accepted for publication. As a service to our customers we are providing this early version of the manuscript. The manuscript will undergo copyediting, typesetting, and review of the resulting galley proof before it is published in its final citable form. Please note that during the production process errors may be discovered which could affect the content, and all legal disclaimers that apply to the journal pertain.



www.elsevier.com/locate/jtbi

Agent-based simulation of Notch mediated tip cell selection in angiogenic sprout initialisation

Katie Bentley ^{a,*} Holger Gerhardt ^b Paul A. Bates ^a

^a*Biomolecular Modelling Laboratory, Cancer Research UK London Research
Institute, 44 Lincoln's Inn Fields, London, WC2A 3PX, UK*

^b*Vascular Biology Laboratory, Cancer Research UK London Research Institute, 44
Lincoln's Inn Fields, London, WC2A 3PX, UK*

Abstract

Angiogenic sprouting requires functional specialisation of endothelial cells into leading tip cells and following stalk cells. Experimental data illustrate that induction of the tip cell phenotype is dependent on the protein VEGF-A; however, the process of tip cell selection is not fully understood. Here we introduce a hierarchical agent-based model simulating a suggested feedback loop that links VEGF-A tip cell induction with Dll4/Notch mediated lateral inhibition. The model identifies VEGF-A concentration, VEGF-A gradients and filopodia extension as critical parameters in determining the robustness of tip/stalk patterning.

The behaviour of the model provides new mechanistic insights into the vascular patterning defects observed in pathologically high VEGF-A, such as diabetic retinopathy or tumour angiogenesis. We investigate the role of cell morphology in tip/stalk patterning, highlighting filopodia as lateral inhibition amplifiers. The model has been used to make a number of predictions, which are now being tested

experimentally, including: 1) levels of Dll4/VEGFR-2, or related downstream proteins, oscillate in synchrony along a vessel in high VEGF environments; 2) a VEGF gradient increases tip cell selection rate.

Key words: Angiogenesis, Agent-based modelling, Notch, Oscillation, Lateral inhibition

1 Introduction

Angiogenesis is the outgrowth of new blood vessels from pre-existing vessels (Risau, 1997). The development of new vasculature by angiogenesis occurs in two stages. First, a dense, immature, evenly spaced network of new vessels develops by recursive sprouting and fusion of sprouts. Second, the network is remodelled into a mature hierarchically spaced network by adaptive pruning events and blood flow. In this paper we focus on the first stage. Sprouting angiogenesis has recently been shown to be precision guided by growth factor gradients (Gerhardt et al., 2003; Gerhardt and Betsholtz, 2005) and repulsive cues (Lu et al., 2004; Weinstein, 2005). The new sprout is headed by a ‘tip cell’, which responds to VEGF-A stimulation by extending filopodia and migrating towards the signal (Gerhardt et al., 2003). The vessel wall of the sprout usually comprises only one or two ‘stalk’ cells before tip cell fusion takes place. Over time the stalk cells divide in response to VEGF and the sprout elongates (Gerhardt and Betsholtz, 2005). New tip cells are then stimulated within the elongating sprout and the process repeats.

* Corresponding Author, Tel: +44 (0)20 7269 3565, Fax: +44 (0)20 7269 3258

Email addresses: katie.bentley@cancer.org.uk (Katie Bentley),

holger.gerhardt@cancer.org.uk (Holger Gerhardt),

paul.bates@cancer.org.uk (Paul A. Bates).

VEGF-A was recently shown to be sufficient and necessary to induce the tip cell response (Gerhardt et al., 2003). Now several studies have identified that Notch signalling controls tip cell selection (Hellström et al., 2007; Lobov et al., 2007; Suchting et al., 2007); the full mechanism, however, remains unclear. Inhibition of Notch leads to a significant increase in tip cells in both normal and pathological angiogenesis (Hellström et al., 2007; Lobov et al., 2007; Noguera-Troise et al., 2006; Ridgway et al., 2006). Pathological angiogenesis, e.g. in tumours and ocular vasculopathies, often leads to highly aberrant vascular patterning with tortuous, leaky vessels. In tumours this reduces drug delivery and increases metastatic potential (Koganehira et al., 2003; Jain, 2005). Such malformations provide a strong incentive to understand the interactions between tissue environment and endothelial cell-cell communication. Interestingly, partial and full inhibition of Dll4-Notch signalling have been shown to resolve some of the aberrant vascular patterning in both retinal vasculopathy and tumours respectively (Hellström et al., 2007; Noguera-Troise et al., 2006; Ridgway et al., 2006).

Tip cell selection is thought to occur in two stages: 1) VEGF mediated activation of VEGFR-2 receptors leads to up-regulation of the ligand delta-like 4 (Dll4) (Lui et al., 2003); 2) Dll4 mediated activation of Notch1 receptors in a neighbouring cell down-regulates VEGFR-2 receptor expression (Williams et al., 2006; Sainson et al., 2005, 2006). The Notch-Dll4 lateral inhibition generates an alternating pattern of cell fates, a ‘salt and pepper’ pattern (Baron, 2003; Brooker et al., 2006); therefore contrary to most angiogenesis models to date, tip cells are only separated by one or two stalk cells in immature vessels (Figs. 1 and 2). The lateral inhibition mechanism can be reduced to the negative feedback loop shown in Fig. 2(b). In the presence of VEGF the tip cell phenotype may be considered ‘default’, since the inhibited stalk cell fate is ‘acquired’ through lateral inhibition (Collier et al., 1996). Tip cells cannot be adjacent, as one would necessarily be inhibited by the other (Collier et al., 1996). Stalk cells may be adjacent provided that at least one neighbour is a tip

cell, otherwise it would receive no inhibition and default back to the tip cell fate.

Filopodia are long thin, dynamic, membrane protrusions; they extend and retract. The retraction of filopodia acts as an efficient search strategy, allowing the cell to optimally redirect its filopodia (Carmeliet, P. and Tessier-Lavigne, 2005). We assume the filopodia are generated by similar pathways to those in fibroblast cells, where a chemoattractant triggers actin recruitment to the site of receptor activation, via proteins WASP and PIP2 (Holt and Koffer, 2001; Bray, 2001). Actin polymerises into filaments which are bundled in parallel pushing out the membrane. Filaments are polarised and highly dynamic, as actin adds onto one end and disassociates from the other. Filopodia retract if the addition rate falls, caused by loss of receptors or chemoattractant.

Computational models have been used to investigate a wide range of blood vessel behaviour (Bartha and Rieger, 2006; Anderson and Chaplain, 1997; Levine et al., 2002; McDougall et al., 2005; Merks and Glazier, 2006). However, many angiogenesis models work at the macro-scale, simulate the effects of multiple factors, and focus on the later stages of angiogenesis such as blood flow (Stephanou et al., 2006; McDougall et al., 2002). A few studies have focused on modelling single aspects at greater resolution, such as the binding of VEGF to VEGFR-2 (Mac Gabhann et al., 2005) showing that processes taken for granted in other models have their own interesting dynamics and stochasticity. Levine et al. (2001) modelled the onset of capillary formation, but with a focus on the role of degradation of the basal lamina and without considering dll4-notch selection or morphological effects, central in our model. The majority of angiogenesis models to date have used continuous methods with the exception of Anderson and Chaplain (1998), where a hybrid model incorporating continuous chemicals with discrete cells was implemented in 2D. Some cellular automata models follow a similar approach to ours: the Epitheliome project, which uses agents to model epithelial cells, (Walker et al., 2004); Merks and Glazier (2006)

neo-vascularisation model; and the Peirce et al. (2004) investigation of pericytes in angiogenesis.

In this paper we aim to understand, through a unique, hierarchical agent based modelling approach, how Notch-mediated selection of tip cells is affected by different VEGF environments and filopodia dynamics. We propose that the characteristically high VEGF observed in vascular pathologies may corrupt the Notch-driven selection of tip cells leading to excessive branching. We consider the novel viewpoint that filopodia play a significant role in selection as an amplifier. Cells that bind more VEGF extend more filopodia. Due to increased surface area they can then bind more VEGF, thus creating a positive feedback that consolidates the tip cell fate. This paper also represents the first step in a larger project to understand how migration, division and anastomosis affect tip cell selection.

In the next section the model will be fully introduced. Agents in the model are altered via interaction with their local environment only (such as neighbouring agents and signalling gradients). Global phenomena such as cell fates, selection rates and vessel patterning *emerge* from the large numbers of agents interacting locally. A number of simulation results will be presented in section 3. An analysis of the mechanistic aspects of selection is given, leading to predictions for subsequent *in vivo* experiments; importantly, we find a possible role for gradients in determining tip cell selection rate and theorise an oscillation of cell fates in high VEGF.

2 Model overview

The model consists of a single hollow, cylindrical capillary comprising ten endothelial cells ('EC agents'). There is one cell per vessel cross section with no autocellular junction (Levine et al., 2001; Uv et al., 2003). For capillary dimensions and initial parameter settings see Fig. 3 and Table 1. Each cell is comprised of smaller 'memA-

agents' on its periphery, representing sections of the membrane (Fig. 4). The surrounding environment contains a fixed distribution of VEGF, similar to the method adopted by Bartha and Rieger (2006). The model is defined over a 3D gridded lattice where each unit of cubic volume ('grid site') has sides of length $0.5 \mu\text{m}$. The memAgents each solely occupy one grid site, unless they belong to a filopodium. Being very thin, filopodia may share a grid site with other filopodia and/or VEGF (see Fig. 5). Thus EC agents extend across many grid sites, similar to a grouped lattice cellular automata (Chen et al., 2006). Each memAgent contains unique levels of Notch1, Dll4 and VEGFR-2 receptors. Each EC agent has knowledge of the total protein levels and activity across its memAgents (Fig. 4). The agents are initialised with internal parameter settings as detailed in Tables 2 and 3. In order to maintain focus on the lateral inhibition mechanism, EC agents are capable of only two actions, extension and retraction of filopodia. Both actions are executed locally by the memAgents. See Fig. 6 for a pseudocode overview of the model.

VEGF concentrations *in vivo* are notably difficult to determine (Mac Gabhann et al., 2005). It is assumed that under normal angiogenic conditions, approximately less than 3% of VEGFR-2 receptors would be bound by VEGF (Mac Gabhann and Popel, 2006); we set the VEGF concentration per grid site such that this assumed occupancy was, on average, attained. Two types of VEGF environment were modelled: 1) uniform VEGF, representing the diffusible isoform VEGF₁₂₀, which had 0.8 molecules per environment grid site; 2) a linearly increasing gradient, representing the ECM binding isoform VEGF₁₆₄, with 0.04 VEGF molecules multiplied by the grid site's position on the y axis (Fig. 3).

2.1 VEGFR-2 and Notch responses

VEGF activation of VEGFR-2 generates two responses in the model: (1) up-regulation of Dll4, via alterations in gene expression (executed during the EC agent update, described in section 2.3) and (2) filopodia extension via actin activation. A memAgent's active VEGFR-2 receptor level V'_m is given by

$$V'_m = V_{sink} V_m M_{tot} / V_{max} \sum_{n=1}^{26} E_n \cdot \text{VEGF}. \quad (1)$$

V'_m is dependent on the sum of VEGF in its local neighbourhood (nearest orthogonal and diagonal grid sites). The constant V_{sink} refers to the number of VEGFR-1 receptors, which act as a sink, removing VEGF from the system (Waltenberger et al., 1994; Hiratsuka et al., 1998). M_{tot} is the current total number of memAgents in the given EC agent.

The EC agent Notch level was constant, representing a balanced rate of degradation and expression, focusing the model on Dll4 dynamics. Notch is activated by Dll4 on a neighbouring cell; both proteins are clustered to the cell-cell junctions. Notch is activated by removal of Dll4 from neighbouring memAgents not belonging to the same cell up to the value of N_m , then $N'_m = N_m$ (refer to Table 3). If less Dll4 exists in its local neighbourhood than N_m then N'_m is set to the total Dll4 available.

2.2 Filopodia

Each memAgent has the potential to extend a single filopodium, provided that the cell's arbitrary membrane stretch limit (M_{max}) has not been reached. It must recruit enough actin to extend (t_{ext}), modelled by the accumulation of actin tokens; see Tables 1 and 3. Actin levels are incremented in a probabilistic fashion dependent

on VEGFR-2 activation, as follows

$$p(\text{actin}) = CV'_m M_{tot} / V_{max}, \quad (2)$$

where C is the intracellular signal strength representing levels of WASP/PIP2 activation. Filopodia are extended by creating a new, linked memAgent within the local grid site neighbour with the highest VEGF level (randomly chosen if no clear highest exists). MemAgents have a state representing their location in filopodia: tip, stalk, base or none (see Fig. 5). When awarded a token, MemAgents not in a filopodium (state ‘none’) pass it to local base state neighbours within a $2 \mu\text{m}$ radius, biasing recruitment to already growing filopodia. Actin is also passed up filopodia, by base and stalk state memAgents, towards the tip. Only tip and none state memAgents can use their actin to extend. Upon extension actin level is reduced by t_{ext} . This system incorporates elements of the more detailed ‘Artificial Cytoskeleton’ model (Bentley and Clack, 2004, 2005).

Filopodia retract if a memAgent in tip state fails to extend for f_{max} time steps; it is then deleted. Upon deletion all proteins are passed backwards to the previous memAgent in the filopodium, which then changes state to become the filopodium tip. This deletion process continues every time step until the base is reached, which instead of being deleted has its status reset to ‘none’. The process of passing proteins backwards during retraction results in a pool of actin accumulating at the old base position. It was assumed that, given receptor activation and sufficient actin, re-extension might occur from that location before the pool could be recruited to an existing filopodium two microns away. Thus memAgents with a retracted actin pool can override the otherwise enforced two micron distance for extension. The actual number of filopodia per EC agent is dynamic and determined each time step by the current conditions, though the maximum possible per cell was 160.

The maximum speed at which a filopodium in the model can extend is by one

memAgent per time step (as newly created memAgents are not updated until the next time step); thus to extend 10 μm would take a minimum of 20 time steps. It would then take f_{max} time steps before taking a further 20 time steps on average to retract. As the experimental data in Leslie and Lewis (2007) indicate, filopodia take a range of times to extend and collapse, the fastest being between 15 and 18 minutes for a 10 micron long filopodium. Taking 18 minutes as a baseline, and setting f_{max} to 30 gives one time step as 15 seconds in the model.

2.3 EC agent update

After all memAgents have updated, each EC agent sums its memAgent's active receptor levels V'_c and N'_c . After a delay, D1 for V'_c and D2 for N'_c (see Fig.2) these levels are effective (V''_c and N''_c) and used in equations 3 and 4 to determine the new cell wide levels of Dll4 and VEGFR-2, which are then divided back out to the memAgents (Dll4 only between junction memAgents). The delays were set such that their sum was approximately 15 minutes, fitting with a similar Notch-delta system (Guidicelli and Lewis, 2004). It was assumed that recovery delays would be very short compared with the time it takes for active receptors to affect transcription. For simplicity R1 and R2 were set to 1 time step, and D1 and D2 were set to 28 time steps.

$$D_{ct} = D_{ct} + V''_c \delta \quad (3)$$

$$V_{ct} = V_{max} - N''_c \sigma \quad (4)$$

2.4 Evaluation

The resulting patterns of primary and secondary cell fates were evaluated at the final time step of the simulation (t_{max}) with regard to three separate factors (1)

the number of tip cells, (2) whether the salt and pepper pattern has been reached and (3) how long the pattern has been stable for.

Tip Cells: A tip cell is defined by the following two criteria, which mean it has filopodia and has not been inhibited: 1) $V_c \geq V_{max}/2$ and 2) $M_{tot} \geq 1.2 \times M_{init}$

Pattern: A score of 1 was given if no tip cells were adjacent and exactly four or five tip cells existed, otherwise a score of zero was given. Note that a zero score does not indicate to what extent the system has failed to generate the pattern. This score was then expressed as a percentage.

Stability: A binary score was given each time step for each EC agent. It would score 1 if $V_{ct} = V_{ct-1} \pm \rho$, and zero otherwise, where ρ was a significance value. At t_{max} the number of consecutive positive scores, working backwards, was averaged over each EC agent and given as a percentage of t_{max} .

3 Results

To assess the effects of VEGF environment on tip/stalk patterning, a number of different simulations were performed. First the effects of a gradient were investigated.

3.1 VEGF gradient affects selection rate

The model was run in both the uniform and linearly increasing VEGF environments. In uniform VEGF it took an average of 720 time steps to achieve a salt and pepper pattern, over 50 runs (stability score of 52%, when $t_{max} = 1500$). In the linear gradient it took less time, 585 time steps on average (a stability score of 61% over 1500 time steps). Fig. 7 shows EC agent morphology differed markedly in the two environments (see supplementary material for movies of typical simulation runs).

In uniform VEGF, curled filopodia grew in random directions compared to long directed filopodia in the linear gradient, consistent with observations in Gerhardt et al. (2003). On average twenty long filopodia were observed per EC agent in the gradient compared to fifty in the uniform VEGF distribution, matching experimental data in retinal angiogenesis (Gerhardt et al., 2003). The increased selection rate in the presence of a gradient can be attributed to filopodia extension. Slight differences in filopodia length between cells can result in large differences in receptor activation if the VEGF distribution is heterogeneous, allowing one cell to gain an advantage more quickly. Thus we predict that *in vivo* the pattern will stabilise faster in the presence of a gradient.

3.2 VEGF concentration affects number of tip cells

The concentration of the uniform VEGF distribution was varied. For each setting of VEGF, between 0.1 and 1.6 molecules per grid site (in intervals of size 0.1) the model was run 50 times, each for 1500 time steps, and scoring results averaged. Figure 9(a) shows that low VEGF yielded a stable arrangement of no tip cells, as not enough VEGF was present to evoke a response. A range of values between 0.5 and 1.2 VEGF molecules per grid site could generate the salt and pepper pattern. With higher VEGF levels beyond this ‘window’ of normal patterning, the cells oscillated in synchrony between all tip cells and all stalk cells, never stabilising into the salt and pepper pattern (Fig. 9). Genetic studies have shown that the levels of VEGF require tight control during normal development as a 50% reduction or doubling in the amount of VEGF leads to severe vascular defects and embryonic lethality (Carmeliet et al., 1996; Ferrara et al., 1996; Miquerol et al., 2000). Interestingly our present results indicate that the process of tip cell selection is strongly influenced by VEGF levels. Only a small range of VEGF concentrations yield normal tip-stalk patterning, which we therefore predict could account, at least in part, for some of

the problems in angiogenesis in high VEGF environments.

3.2.1 *Oscillation in high VEGF*

For the oscillation of cell fates to occur in synchrony across all EC agents, adjacent cells must consistently inhibit each other fully, with no room left for one to gain an inhibitory advantage. In very high VEGF this is conceivable as enough receptors are activated to maximally inhibit neighbours, thus further outgrowths of filopodia can yield no further inhibition. When fully inhibited EC agents cannot continue production of Dll4 and so cannot maintain inhibition, thus causing an oscillation (Fig. 2(b)). The oscillation predicted by our model has never before been proposed for this system; it is as yet undiscovered in the laboratory. However, in other systems oscillating negative feedback-loops are fundamental. For example, the segmentation clock in developing vertebrates utilises negative feedback oscillations to control the spacing of somites (Guidicelli and Lewis, 2004). A similar negative feedback simulation has also been shown to induce oscillations when activation levels are high (Di Ventura et al., 2006).

In Fig. 10 we present observational data which shows the oscillation to be plausible. Fig. 10(a) shows one vessel region comprised entirely of tip cells and Fig. 10(b) shows another region of the same retina comprised entirely of stalk cells. These ‘patches’ are an as yet unexplained phenomenon observed in retinal vessels exposed to pathologically high VEGF (Hellström et al., 2007). Interestingly, in light of the oscillation predicted by the model, the patches could be accounted for as different regions of synchronously oscillating cells captured out of phase in one still image. One would expect the regions to be out of phase as the vessels themselves will have formed at different times.

The oscillation has a number of implications. If the patches explanation is correct, it

could account for abnormal vessel dilation and excessive branching in pathological angiogenesis. However, our model is simple and so it is feasible that pathways not included have evolved to dampen the oscillation or force the system to chose one particular fate. It has also been noted that for oscillations to occur, the lifetime of molecules involved must be short compared with the sum of transcriptional delays (Guidicelli and Lewis, 2004). With these considerations in mind, experiments are now underway to investigate its existence.

The period of the oscillation was found to be 116 time steps (29 minutes). This is consistent with the period observed in (Guidicelli and Lewis, 2004) and their equation showing oscillation period is equal to twice the sum of the transcriptional delays. In our model, twice the sum of delays does indeed give the period $((28+28+1+1) \times 2)$. To test if the delay-period relationship still held true with different delay settings, the model was run fifty times for each setting between 10 and 50 (in intervals of size 10) for both delays $D1$ and $D2$. Each run lasted 3000 time steps, accommodating the larger delay settings. Fig. 11(a) shows results where $D1 = D2$, but the same relationship held true for $D1 < D2$ and $D1 > D2$. Thus the sum of the delays is more important than their particular values.

3.3 *Dll4 under and over expression*

The δ parameter, which controlled the expression level of $Dll4$ in response to VEGF (see Fig. 2), was varied. Setting δ to 1 is equivalent to a $Dll4^{+/-}$ heterozygous knockout genotype (as δ was set to 2 in the normal case). For each δ setting between zero and four (in 0.2 intervals) the model was run 50 times, each for 1500 time steps. Averaged results are shown in Fig. 8(b). Again a viable window for normal patterning is clear after which oscillation is observed. However, in contrast to Fig. 8(a) low levels of $Dll4$ are associated with too many tip cells due to a lack of

inhibition into the secondary cell fate rather than a lack of VEGF.

Fig. 8(b) shows that in the model a $Dll4^{+/-}$ knockout is unable to stabilise into the salt and pepper pattern. The lowered inhibition level causes all cells to be classified as tip cells, the default fate. This is consistent with experimental observations where heterozygous knockout mice still have some Notch activity but produce too many tip cells (Hellström et al., 2007), as shown in Fig. 11(c). Sainson et al. (2005) observed more tip cells when Notch signalling was inhibited *in vitro* and attributed this to increased tip cell proliferation. However *in vivo* tip cells rarely divide (Gerhardt et al., 2003). Instead, the increased number appears to be due to adjacent tip cells not inhibiting each other fully.

3.4 Phase Plane Analysis

To give greater insight into how relative strengths of each model aspect contribute to a given behaviour, a phase plane analysis was performed. Thus, the three aspects of the system: filopodia dynamics, lateral inhibition and VEGF environment, were varied against each other. It was desirable to dedimensionalise the system and only vary three parameters, one for each aspect of the system. All simulations were run in the uniform VEGF environment, varying just the concentration. The constant C in equation 2 controlled filopodia dynamics; increases in C raise the chance of extension. Only δ (Fig. 2) was varied to control lateral inhibition. σ was not varied as it was found that the product of δ and σ was more important than their actual values. To gain a broad view the following parameter settings were used: $\delta, C \in \{0, 1, 2, 3, 4\}$ and $VEGF \in \{0.4, 0.8, 1.2, 1.6\}$ (molecules per grid site). For each combination of parameter settings the model was simulated fifty times, each for 1500 time steps. The average system behaviour was then classed as one of the following four types of behaviours (phases).

Phase 1 No response: tip cells score < 4 , stability score > 50 , pattern score = 0

Phase 2 No inhibition: tip cells score > 5 , stability score > 50 , pattern score = 0

Phase 3 Salt and pepper pattern: tip cells score = 4 or 5, pattern score = 1

Phase 4 Oscillation: stability score < 5 , pattern score = 0

The diagrams in Fig. 8(c) show there are two approaches for returning an oscillating system to phase 3 normal patterning when in high VEGF (e.g. VEGF = 1.6): 1) change the environment or 2) change the cell's *perception* of the environment. The latter can be achieved by 'turning down' lateral inhibition, via δ , making the cells react as if there is less VEGF. Phase 3 was achieved at around half the original value of δ , which is understandable as the environment contained $2 \times$ VEGF. The prediction from these results suggests that a Dll4^{+/-} mutant would perform normal patterning in twice the VEGF level; experiments are now underway to test this *in vivo*. The diagrams also show that if C is reduced alongside δ then there are more viable settings of δ that will achieve phase 3 behaviour; both EC agent's perceptual channels have been manipulated. However, reducing C alone does not yield phase 3, the lateral inhibition must be reduced to avoid oscillation.

Interestingly, in the uniform environment it was found that reducing δ could not generate normal patterning in greater than $2 \times$ VEGF. The same test was run in the linear gradient with results averaged over 50 runs of 3000 time steps. The VEGF level in each grid site was multiplied by a scalar x (ranging from 2 to 10 times normal VEGF (0.8)). For each VEGF setting, δ was divided by x . Results in Fig. 11(b) show that phase 3 could be achieved at higher than $2 \times$ VEGF. Stability was inversely proportional to VEGF level. This result has interesting implications, suggesting once again that gradient rather than concentration could be a key factor in the success of achieving the salt and pepper pattern. Reducing C by the same factor alongside δ up to $20 \times$ VEGF, yielded phase 3 and consistently high stability

for every x setting.

4 Discussion and conclusions

The model has reproduced many experimentally observed aspects of tip cell selection. Loss of Dll4 leads to increased tip cell density. Uniform VEGF distribution leads to curly and more numerous filopodia, whereas gradients lead to longer more directed filopodia. Lateral inhibition via Notch generates a salt and pepper pattern under normal angiogenic conditions. Excessive tip cells are observed in high VEGF and a ‘normalisation window’ was observed across different combinations of parameters. The model, validated by these qualitative similarities to experimental observations, has been used to make a number of predictions, which are now being tested. Specifically: (1) the salt and pepper pattern will stabilise faster in VEGF gradients than in uniform environments due to filopodial amplification, (2) levels of Dll4/VEGFR-2 or related downstream proteins will oscillate in synchrony along a vessel in high VEGF.

It was shown by removing all environmental and internal cell biasing, that the Notch-Dll4 lateral inhibition mechanism can generate the salt and pepper pattern of normal tip cell selection. Therefore, abnormal patterning can be attributed to the dynamics of this particular system, rather than any uncontrolled bias. However, heterogeneity in the environment and cell protein levels no doubt serve to improve the robustness of this system, conferring an advantage to certain cells without independently causing the selection. The protein levels used did not necessarily reflect the actual protein numbers, but rather the amounts that are available for activation, simulating the net effect of many interactions between cofactors.

Our phase-plane diagram implies that lateral inhibition needs to be ‘turned down’ in high VEGF environments. This may initially seem counter intuitive: as more tip

cells are observed in high VEGF we might expect to need to turn up the lateral inhibition. This result, however, is reinforced by the evidence in Hellström et al. (2007) that inhibition of Notch signalling in retinal vasculopathy helped renormalise tip cell numbers. It also showed that combining a reduction in notch activity with a reduced filopodial response may improve robustness of the patterning.

The model was designed as a hierarchical agent model to facilitate subsequent extensions, such as cell migration, cell division and anastomosis through realistic modelling of cell shape changes. This modelling approach focuses on the emergence of whole-system behaviours and complex shapes from local lower-level environment-system interactions. We expect that experiments currently underway to test the model predictions will highlight aspects for further refinement. Through such model-test-refine loops we aim to edge closer to a more complete understanding of tip cell dynamics and their potential role as a therapeutic target in pathological angiogenesis.

5 Acknowledgements

The work was funded by Cancer Research UK and the authors would like to thank the Biomolecular Modelling Laboratory for helpful discussions and manuscript editing. We are grateful to Thomas Hegendoerfer and Jon Leslie for sharing unpublished data on the dynamics of filopodia extension in live zebrafish.

References

Anderson, A. R. A., Chaplain, M. A. J. 1997. A Mathematical Model for Capillary Network Formation in the Absence of Endothelial Cell Proliferation. *App. Math. Letters*. 11, 109-114.

- Anderson, A. R. A., Chaplain, M. A. J. 1998. Continuous and Discrete Mathematical Models of Tumour-Induced Angiogenesis. *Bull. Math. Biol.* 60, 857-899.
- Baron, M. 2003. An Overview of the Notch Signalling Pathway. *Seminars in Cell & Developmental Biology.* 14, 113-119.
- Bartha, K., Rieger, H. 2006. Vascular network remodelling via vessel cooption, regression and growth in tumours. *J. Theor. Biol.* 241(4), 903-918.
- Bentley, K., Clack, C. 2004. The Artificial Cytoskeleton For Lifetime Adaptation of Morphology. In Bedau, M. et al. (eds.). *Workshop Proc. of the 9th Int. Conf. on the Simulation and Synthesis of Living Systems*, pp 13-16.
- Bentley, K., Clack, C. Morphological plasticity: environmentally driven morphogenesis. 2005. In Capcarrere. M. S., Freitas. A. A., Bentley. P. J., Johnson. C. G., Timmis. J. (Eds.). *Proceedings of the 8th European Conference on Artificial Life (ECAL)*. Springer Verlag, pp.118-127.
- Bray, D. 2001. *Cell Movements: From Molecules to Motility*. Garland Science. 2nd Edition.
- Brooker, R., Hozumi, K., Lewis, J. 2006. Notch ligands with contrasting functions: jagged1 and delta1 in the mouse inner ear. *Development.* 133, 1277-1286.
- Carmeliet, P., Ferreira, V., Breier, G., Pollefeyt, S., Kieckens, L., Gertsenstein, M., Fahrig, M., Vandenhoek, A., Harpal, K., et al. 1996. Abnormal blood vessel development and lethality in embryos lacking a single VEGF allele. *Nature.* 380, 435-9.
- Carmeliet, P., Tessier-Lavigne, M. 2005. Common mechanisms of nerve and blood vessel wiring. *Nature.* 436, 193-200.
- Chen, C-C., Nagl, S., Clack, C. 2006. Computational techniques for modelling and simulating biological systems. *ACM Computing Surveys.* 34(3), 1-36.
- Collier, J. R., Monk, N. A. M., Maini, P. K., Lewis, J. 1996. Pattern formation by lateral inhibition with feedback: a mathematical model of Delta-Notch intercellular signalling. *J. Theor. Biol.* 183, 429-446.

- Di Ventura, B., Lemerle, C., Michalodimitrakis, K., Serrano, L. From *in vivo* to *in silico* biology and back. *Nature*. 443(5), 527-533.
- Ferrara, N., Carver-Moore, K., Chen, H., Dowd, M., Lu, L., O'Shea, K. S., Powell-Braxton, L., Hillan, K. J., Moore, M. W. 1996. Heterozygous embryonic lethality induced by targeted inactivation of the VEGF gene. *Nature*. 380, 439-442.
- Freitas Jr, R. A. 1999. *Nanomedicine. I: Basic Capabilities*. Landes Bioscience. Georgetown. TX.
- Gerhardt, H., Golding, M., Fruttiger, M., Ruhrberg, C., Lundkvist, A., Abramsson, A., Jeltsch, M., Mitchell, C., Alitalo, K., Shima, D., Betsholtz, C. 2003 VEGF guides angiogenic sprouting utilizing endothelial tip cell filopodia. *Journal of Cell Biology*. 161(6), 1163-1177.
- Gerhardt, H., Betsholtz, C. 2005. How do endothelial cells orientate? In Clauss. M. and Breier. G.(Eds.) *Mechanisms of Angiogenesis*. EXS(94), pp. 3-16.
- Guidicelli, F., Lewis, J. 2004. The vertebrate segmentation clock. *Current Opinion in Genetics & Development*. 14, 407-414.
- Hellström, M., Phng, L-K., Hofmann, J. J., Wallgard, E., Coultas, L., Lindblom, P., Alva, J., Nilsson, A. K., Karlsson, L., Gaiano, N., Yoon, K., Rossant, J., Iruela-Arispe, M. L., Kalen, M., Gerhardt, H., Betsholtz, C. 2007. Dll4 signalling through Notch1 regulates formation of tip cells during angiogenesis. *Nature*. 445(7129), 722-3.
- Hiratsuka, S., Minowa, O., Kuno, J., Noda, T., Shibuya, M. 1998. Flt-1 lacking the tyrosine kinase domain is sufficient for normal development and angiogenesis in mice. *Proc. Natl. Acad. Sci. U. S. A.* 95, 9349-9354.
- Holt, M. R., Koffer, A. Cell motility: proline-rich proteins promote protrusions. *TRENDS in Cell Biology*. 11(1), 38-46.
- Jain, R. K. 2005. Normalization of tumour vasculature: an emerging concept in antiangiogenic therapy. *Science*. 307, 58-62.
- Koganehira, Y., Takeoka, M., Ehara, T., Sasaki, K., Murata, H., Saida, T.,

- Taniguchi, S. 2003. Reduced expression of actin-binding proteins h-caldesmon and calponin h1 in the vascular smooth muscle inside melanoma lesions: an adverse prognostic factor for malignant melanoma. *Br J Dermatol.* 148(5), 971-980.
- Leslie, J. D., Ariza-McNaughton, L., Bermange, A. L., McAdow, R., Johnson, S. L., Lewis, J. 2007. Endothelial signalling by the Notch ligand Delta-like 4 restricts angiogenesis. *Development.* 134(5), 839-844.
- Levine, H. A., Sleeman, B. D., Nilson-Hamilton, M. 2001. Mathematical modelling of the onset of capillary formation initiating angiogenesis. *Journal of Mathematical Biology.* 42, 195-238.
- Levine, H. A., Tucker, A. L., Nilson-Hamilton, M. 2002. A Mathematical model for the role of cell signal transduction in the initiation and inhibition of angiogenesis. *Growth Factors.* 20, 155-175.
- Lobov, I. B., Renard, R. A., Papadopoulos, N., Gale, N. W., Thurston, G., Yancopoulos, G. D., Wiegand, S. J. 2007. Delta-like ligand 4 (Dll4) is induced by VEGF as a negative regulator of angiogenic sprouting. *Proc. Natl. Acad. Sci. U S A.* 104(9), 3219-24.
- Lu, X., le Noble, F., Yuan, L., Jiang, Q., de Lafarge, B., Sugiyama, D., Bréant, C., Claes, F., De Smet, F., Thomas, J-L., Autiero, M., Carmeliet, P., Tessier-Lavigne, M., Eichmann, A. 2004. The netrin receptor UNC5B mediates guidance events controlling morphogenesis of the vascular system. *Nature.* 432, 179-186.
- Liu, Z-J., Shirakawa, T., Li, Y., Soma, A., Oka, M., Dotto, P., Fairman, R., Velazquez, O.C., Herlyn, M. 2003. Regulation of *Notch1* and *Dll4* by Vascular Endothelial Growth Factor in Arterial Endothelial Cells: implications for modulating arteriogenesis and angiogenesis. *Molecular and Cellular Biology.* 23(1), 14-25.
- Mac Gabhann, F., Popel, A. S. 2004. Model of competitive binding of vascular endothelial growth factor and placental growth factor to VEGF receptors on endothelial cells. *Am J Physiol Heart Circ Physiol.* 286, 153-164.

- Mac Gabhann, F., Yang, M. T., Popel, A. S. 2005. Monte Carlo Simulations of VEGF binding to cell surface receptors *in vitro*. *Biochimica et Biophysica Acta*. 1746, 95-107.
- Mac Gabhann, F., and Popel, A. S. 2006. Computational Model of Vascular Endothelial Growth Factor Spatial Distribution in Muscle and Pro-Angiogenic Cell Therapy. *Plos Comput. Biol.* 2(9), 1107-1120.
- McDougall, S. R., Anderson, A. R. A., Chaplain, M. A. J., Sherratt, J. A. 2002. Mathematical modelling of flow through vascular networks: implications for tumour-induced angiogenesis and chemotherapy strategies. *Bull. Math. Biol.* 64, 673-702.
- McDougall, S. R., Anderson, A. R. A., Chaplain, M. A. J. 2006. Mathematical modelling of dynamic adaptive tumour-induced angiogenesis: Clinical implications and therapeutic targeting strategies. *J. Theor. Biol.* 241(3), 564-589.
- Merks, R. M. H., Glazier, J. A. 2006. Dynamic mechanisms of blood vessel growth. *Nonlinearity*. 19, C1-C10.
- Miquerol, L., Langille, B. L., Nagy, A. 2000. Embryonic development is disrupted by modest increases in vascular endothelial growth factor gene expression. *Development*. 127, 3941-3946.
- Noguera-Troise, I., Daly, C., Papadopoulos, N. J., Coetzee, S., Boland, P., Gale, N. W., Lin, H. C., Yancopoulos, G. D., Thurston, G. 2006. Blockade of Dll4 inhibits tumour growth by promoting non-productive angiogenesis. *Nature*. 444, 1032-1037.
- Peirce, S. M., Van Gieson, E. J., Skalak, T. C. 2004. Multicellular simulation predicts microvascular patterning and *in silico* tissue assembly. *FASEB J.* 18, 731-733.
- Ridgway, J., Zhang, G., Wu, Y., Stawicki, S., Liang, W-C., Chanthery, Y., Kowalski, J., Watts, R. J., Callahan, C., Kasman, I., Singh, M., Chien, M., Tan, C., Hongo, J-A. S., de Sauvage, F., Plowman, G., Yan, M. 2006. Inhibition of Dll4 signalling inhibits tumour growth by deregulating angiogenesis. *Nature*. 444, 1083-1087.

- Risau, W. 1997. Mechanisms of angiogenesis. *Nature*. 386. 671-674.
- Sainson, R., Aoto, J., Nakatsu, M. N., Holderfield, M., Conn, E., Koller, E., Hughes, C. C. W. 2005. Cell-autonomous Notch signalling regulates endothelial cell branching and proliferation during vascular tubulogenesis. *FASEB J.* 19(8), 1027-9.
- Sainson, R. C. A. and Harris, A. L. 2006. Hypoxia-regulated differentiation: let's step it up a Notch. *TRENDS in molecular medicine*. 12(4), 141-143.
- Stephanou, A., McDougall, S., Anderson, A., Chaplain, M.A.J. 2006. Mathematical modelling of the influence of blood rheological properties upon adaptive tumour-induced angiogenesis. *Math. Comp. Modell.* 44, 96-123.
- Suchting, S., Freitas, C., le Noble, F., Benedito, R., Brant, C., Duarte, A., Eichmann, A. 2007. The Notch ligand Delta-like 4 negatively regulates endothelial tip cell formation and vessel branching. *PNAS*. 104, 3225-3230.
- Uv, A., Cantera, R., Samakovlis, C. 2003. *Drosophila* tracheal morphogenesis: intricate cellular solutions to basic plumbing problems. *TRENDS in Cell Biology*. 13(6), 301-309.
- Walker, D. C., Southgate, J., Hill, G., Holcombe, M., Hose, D. R., Wood, S. M., MacNeil, S., Smallwood, R. H. 2004. The Epitheliome: agent-based modelling of the social behaviour of cells. *BioSystems*. 76, 89-100.
- Waltenberger, J., Claesson-Welsh, L., Siegbahn, A., Shibuya, M., Heldin, C. H. 1994. Different signal transduction properties of KDR and Flt1. two receptors for vascular endothelial growth factor. *J. Biol. Chem.* 269, 26988-26995.
- Wang, D., Lehman, R. E., Donner, D. B., Malti, M. R., Warren, R. S., Welton, M. L. 2002. Expression and endocytosis of VEGF and its receptors in colonic vascular endothelial cells. *Am J Physiol Gastrointest Liver Physiol*. 282., 1088-1096.
- Weinstein, B. M. 2005. Vessels and nerves: marching to the same tune. *Cell*. 120, 299-302.
- Williams, C. K., Li, J-L., Murga, M., Harris, A. L., Tosato, G. 2006. Up-regulation

of the Notch ligand delta-like 4 inhibits VEGF induced endothelial cell function. Blood. 107(3), 931-939.

Figure Legends

Fig 1. (a) Representative image of the growing vascular front in a mouse retina at postnatal day 5. Endothelial cells visualized by Isolectin B4 conjugated to AlexaFluor 568 (red). Alternating stretches of leading membrane, with and without filopodia extension, correspond to an alternating pattern of tip (T) and stalk cells (S). Red Macrophage above the vessel labelled M. Arrow points to filopodia still visible on stalk cell, as it is not yet fully inhibited, relating to stage 2 in the schematic below. (b) Combined nuclear DAPI labelling (blue) and endothelial cell junction labelling with VE-cadherin antibodies (green) illustrate that a limited number of endothelial nuclei (stars), which correspond to either tip cells (T) or stalk cells (S), constitute the sprouting front. Nuclei outside vessel belong to astrocytes. (c) High magnification of the tip cell region of a mouse retina from the transgenic Notch reporter line (TNR1, (Hellström et al., 2007)). Active Notch signalling in the stalk cell (S) between two tip cells (T) is indicated by the green GFP signal. Cell nuclei are counter-stained with DAPI (Blue). Dll4 protein labelled red is prominent in the tip cells. Macrophage labelled M. All scale bars are $10\mu\text{m}$. (d) Schematic of tip cell selection initiating sprouting, our model simulates stages 1-3.

Fig 2. (a) The two pathways involved in Notch mediated tip cell fate determination. D1 and D2 are transcriptional delays. R1 and R2 are recovery delays representing the time it takes before gene expression returns to normal. δ and σ represent expression levels in response to receptor activation or loosely, transcription factors. (b) The pathway as a negative feedback loop, active VEGFR-2 (V') induces Dll4 (D), which increases active Notch1 (N') leading to VEGFR-2 inhibition.

Fig 3. Initial model setup. Each small cube that the vessel is made up from is a memAgent. MemAgents at a junction (blue), VEGF (yellow), V_c level is initially at maximum (green). Initial dimensions in Table 1.

Fig 4. (a) Each EC agent is comprised of smaller memAgents, representing sections of the membrane. Each memAgent has its own internal quantities of proteins and the EC agent stores the total quantities. See Tables 2 and 3. (b) Lattice implementation (2D version with circular cells), C = cell interior (inert), M = memAgent, E=environment. The lattice, or grid, representation allows the local neighbourhood of a memAgent to be clearly defined, e.g. the highlighted memAgent on the left will only interact with VEGF in the four nearest environment grid sites.

Fig 5. EC agents extend filopodia by creating new memAgents linked together. The memAgents in filopodia have knowledge of the agents it is linked to above and below, held in its minusSite and plusSite internal knowledge. See Table 3. A memAgent's internal state 'Fstatus' = B (base) if the minusSite is empty, T (tip) if the plusSite is empty and S (stalk) otherwise, indicating where in the filopodia it resides. MemAgents in filopodia, but not at the base, are represented by thinner shapes within environment E state grid sites.

Fig 6. Model pseudo code overview. For every time step upto t_{max} (when the system is evaluated): 1) all memAgents update in random order asynchronously. A memAgent first checks whether it should be deleted, if in a retracting filopodia. If not then it updates its number of active receptors based on the local environment and may be awarded actin. Actin is recruited or spent in extending a filopodia. 2) when all memAgents have been updated, each EC agent updates its active receptor totals and uses them, after a delay, to determine new cell wide levels of Dll4 and VEGFR-2, which are then divided back out to all memAgents.

Fig 7. Screen shots taken when the salt and pepper pattern stabilised (t) in each environment. Colour represents VEGFR-2 levels (V_c) on a continuum scale from purple (low) to green (high). a) Uniform VEGF, $t=1140$. Filopodia grow in all directions and curl randomly, (b) Linear gradient, $t=650$. Filopodia grow straight towards higher VEGF levels at top. EC agents are each $10 \mu\text{m}$ wide. See Fig 3 and Table 1.

Fig 8. Graphs showing model dynamics obtained in a uniform VEGF distribution. Thick line = pattern score, thin line = stability score, dotted line = tip cell score. (a) Varying the VEGF level showed a window of VEGF concentration generating normal tip cell patterning, below this would generate no behaviour and above the system would oscillate. (b) Varying the δ parameter (altering Notch activation via suppression/over expression of Dll4) shows high tip cell numbers were yielded with no lateral inhibition (δ low) and abnormal oscillation in high Dll4 expression. (c) Phase diagram showing how system behaviour varies with changes in VEGF, lateral inhibition (δ) and filopodia dynamics (C). Phase 1: no response (yellow); 2: no inhibition (blue); 3: S&P pattern (green); 4: oscillation (red).

Fig 9. Graphs showing the VEGFR-2 levels in each cell over one run, all in uniform VEGF. (a) normal VEGF level, half the cells stabilise at $t=1001$ into tip cells (high VEGFR-2) and the other half with low VEGFR-2; (b) in twice the VEGF level the cells VEGFR-2 levels are seen to regularly oscillate in synchrony; (c) and (d) show the product of $\delta\sigma$ is important rather than their specific values.

Fig 10. Patches of ‘all tip cells’ along a vessel or ‘all stalk cells’ are representative of vasculature in pathological angiogenesis, which may support the synchronous oscillation predicted by the model. Here, two regions of one representative confocal image of a retina injected with 300ng VEGF-A164 on day 3 and fixed 24h later, are shown with isolectin B4 conjugated to AlexaFluor 568. In a normal retina, as shown in Fig. 1, any chosen region at the leading edge will have filopodia in alternating

positions. But here one region is shown (a) with all tip cells (excessive filopodia and sprouting) and in another region of the same retina (b) no tip cells (no filopodia) can be observed at the leading edge.

Fig 11. (a) Period of oscillation in high uniform VEGF (VEGF= 1.6) correlates with increase in delay parameters D1, D2. (b) Normal patterning in high VEGF in linearly increasing gradient, gained by reducing δ proportionally with VEGF increase. Stability drops as VEGF increases unless C is also reduced proportionally. Thick line = pattern score, thin line = stability score, dotted line = tip cell score. (c) Dynamics of V_c in all EC agents over one run with Dll4^{+/-} mutant ($\delta = 1$). The cells are unable to inhibit each other enough to generate stalk cells.

Supplementary Material A. Simulation in uniform VEGF with normal concentration (0.8 molecules per grid site). Colour represents VEGFR-2 levels (V_c) on a continuum scale from purple (low) to green (high). Salt and pepper pattern takes longer to stabilise than in the presence of a VEGF gradient.

Supplementary Material B. Simulation in linearly increasing VEGF gradient, with normal concentration ($0.04 \times y$ axis position, molecules per grid site). Colour represents VEGFR-2 levels (V_c) on a continuum scale from purple (low) to green (high). Salt and pepper pattern is faster to stabilise than without a gradient.

6 Tables

| Parameter | Definition | Setting | Reference |
|-----------------|--------------------------------|-------------|-----------------|
| X_g, Y_g, Z_g | grid width, length, depth | 200, 76, 20 | model specific |
| C_{tot} | EC agents | 10 | model specific |
| M_{init} | initial memAgents per EC agent | 1288 | calculated |
| w_c | width of EC agents | 20 | (Freitas, 1999) |
| l_v | vessel length | 200 | calculated |
| r_l | radius of lumen | 4 | (Freitas, 1999) |

| | | | |
|------------|-----------------------------------------------|---------------|-----------------------------------------|
| r_v | radius of vessel | 6 | (Freitas, 1999) |
| g | gap between vessel and lattice boundary | 4 | model specific |
| V_{max} | max VEGFR-2 receptors | 46,000 | calculated from (Wang et al., 2002) |
| V_{min} | min VEGFR-2 receptors | 1,000 | estimated |
| N | Notch receptors | 10,000 | estimated |
| D_{max} | max Dll4 | 10,000 | estimated from (Lui et al, 2003) |
| D_{min} | min Dll4 ligands | 0 | estimated |
| f_{max} | max time before memAgent collapses filopodia | 30 | estimated from (Leslie and Lewis, 2007) |
| V_{sink} | proportion of VEGF left by VEGFR-1 | 0.11 | estimated |
| t_{ext} | Actin tokens required for filopodia extension | 3 | estimated |
| M_{max} | max memAgents per EC agent | 1800 | estimated |
| δ | Dll4 expression change due to VEGFR-2 | 2 | estimated |
| σ | VEGFR-2 expression change due to Notch1 | 15 | estimated |
| ρ | significance range for pattern stability | $V_{max}/6.6$ | model specific |
| C | strength of VEGFR-2 intracellular signal | 2 | estimated |
| $VEGF$ | VEGF molecules per grid site | 0.8 | calculated, see text |
| t_{max} | evaluation time step | 1500 | estimated |

Table 1: Model dimensions and parameters, distances given in grid sites (0.5 μm sided cubes), times given in time steps (one time step is 15 seconds).

| Attribute | Description | Setting | Range |
|-----------|--------------------------------|-----------|------------------------------------------------|
| V_c | level of VEGFR-2 | V_{max} | $V_{min} \leq V_c \leq V_{max}, V_c$ |
| V'_c | level of active VEGFR-2 | 0 | $0 \leq V'_c \leq V_{max}, V'_c$ |
| D_c | level of Dll4 | 0 | $D_{min} \leq D_c \leq D_{max}, D_c$ |
| N_c | level of Notch1 | N | $N_c = N$ |
| N'_c | level of active Notch1 | 0 | $0 \leq N'_c \leq N, N'_c$ |
| N''_c | effective active Notch1 | 0 | $0 \leq N''_c \leq (N \times R2), N''_c$ |
| V''_c | effective active VEGFR-2 | 0 | $0 \leq V''_c \leq (V_{max} \times R1), V''_c$ |
| S_t | stability score at time step t | 0 | $S_t \in [0, 1]$ |

Table 2: Initial EC agent internal knowledge settings. See text for explanations.

| Attribute | Description | Setting |
|-----------|-----------------------|-------------------|
| V_m | level of VEGFR-2 | V_{max}/M_{tot} |
| V'_m | level of active VEGFR | 0 |

| | | |
|-------------|-------------------------------------------------------|-------------|
| D_m | level of Dll4 | 0 |
| N_m | level of Notch1 (if $Jstatus = 1$) | N/M_{tot} |
| N'_m | level of active Notch1 | 0 |
| d | indicates if memAgent is in a collapsing filopodia | 0 |
| $Fstatus$ | indicates memAgent's location in a filopodia | none |
| $Jstatus$ | indicates if memAgent resides at a cell-cell junction | 1=yes, 0=no |
| $Tokens$ | no. of actin tokens | 0 |
| $minusSite$ | previous memAgent in filopodia | NULL |
| $plusSite$ | memAgent ahead in filopodia | NULL |

Table 3: Initial memAgent internal knowledge settings. See text for explanations.

Accepted manuscript

Fig 2

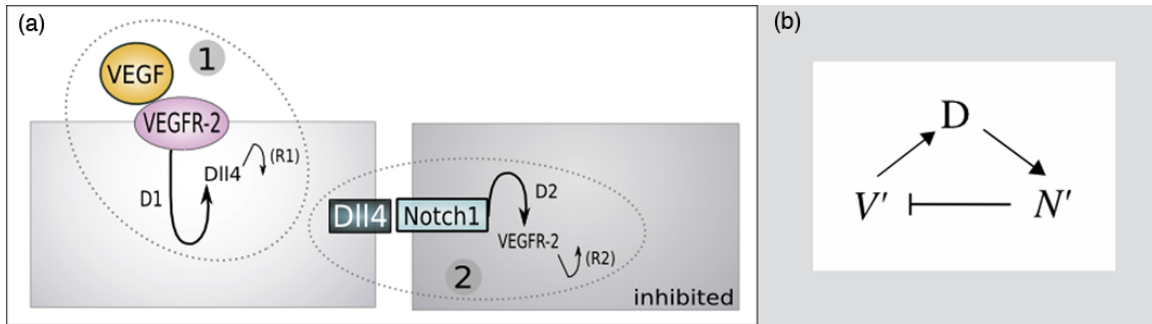
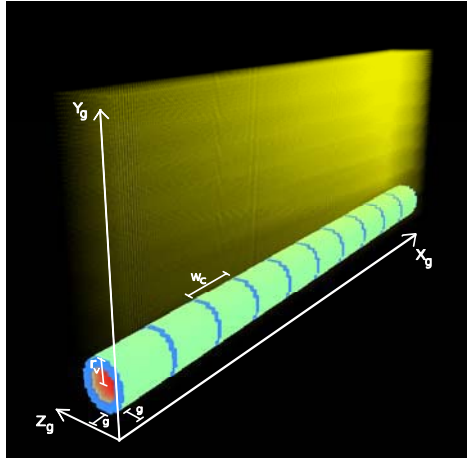
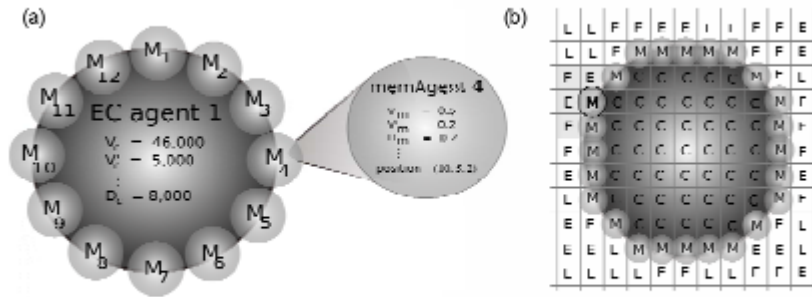


Fig 3



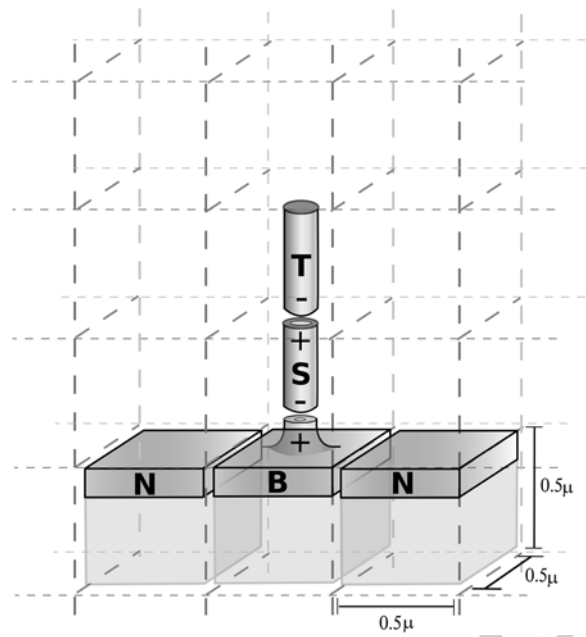
Accepted manuscript

Fig 4



Accepted manuscript

Fig 5



Accepted manuscript

Fig 6

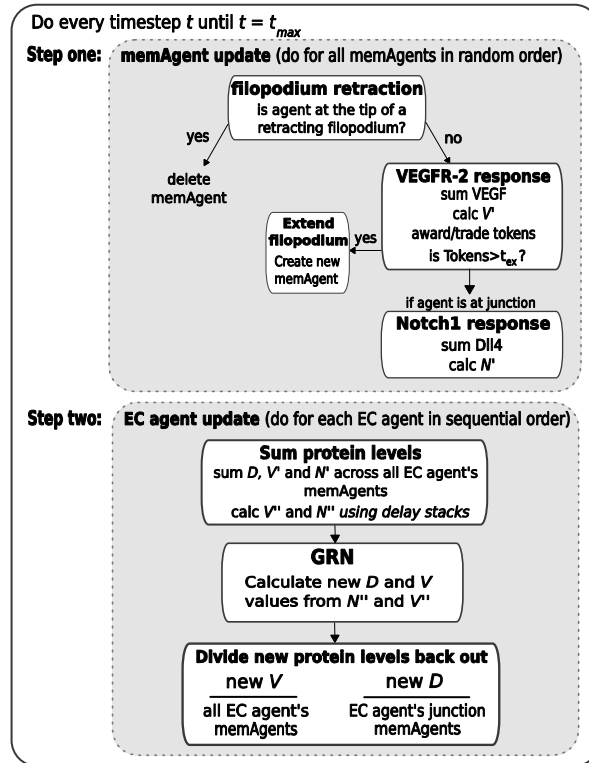


Fig 7

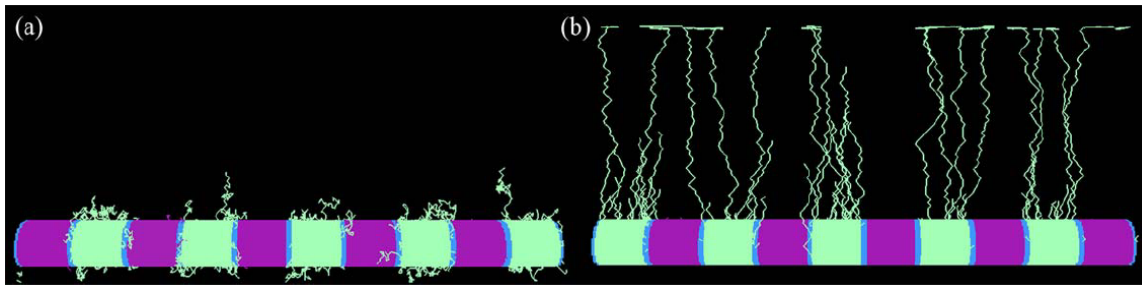


Fig 8

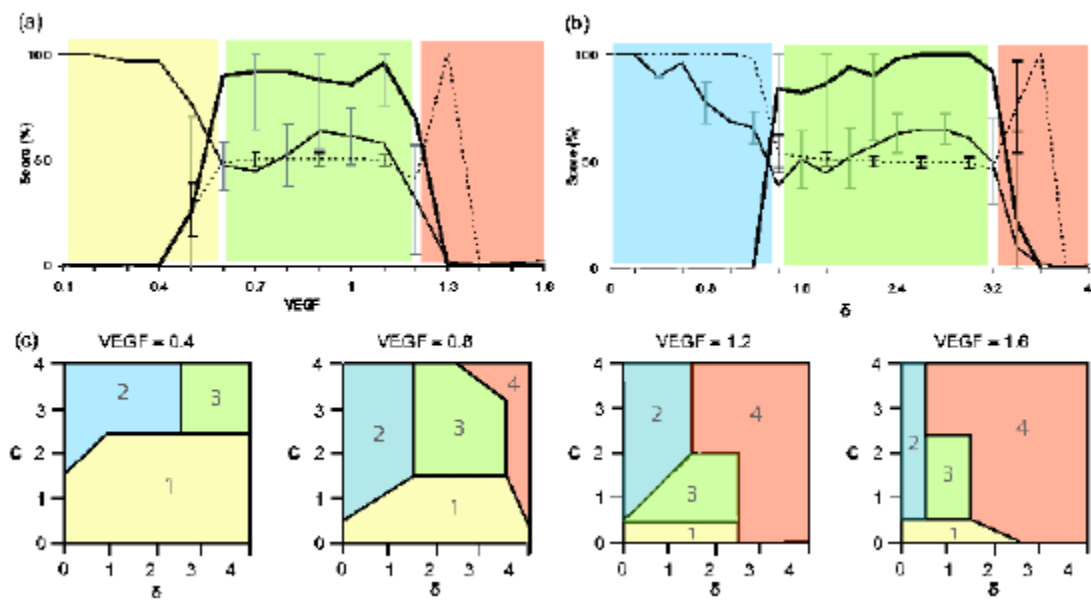


Fig 9

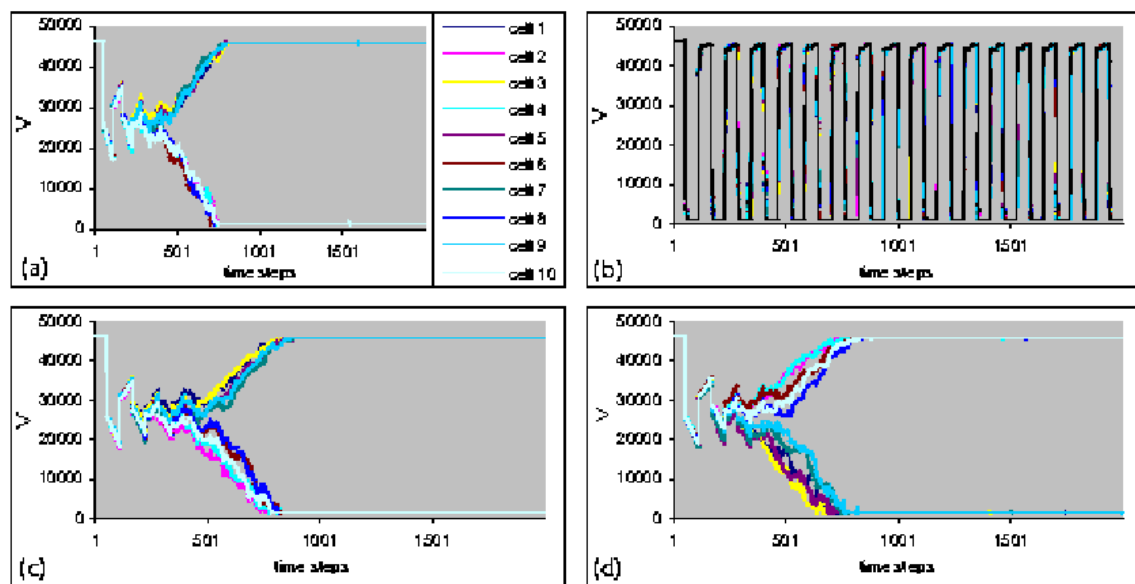
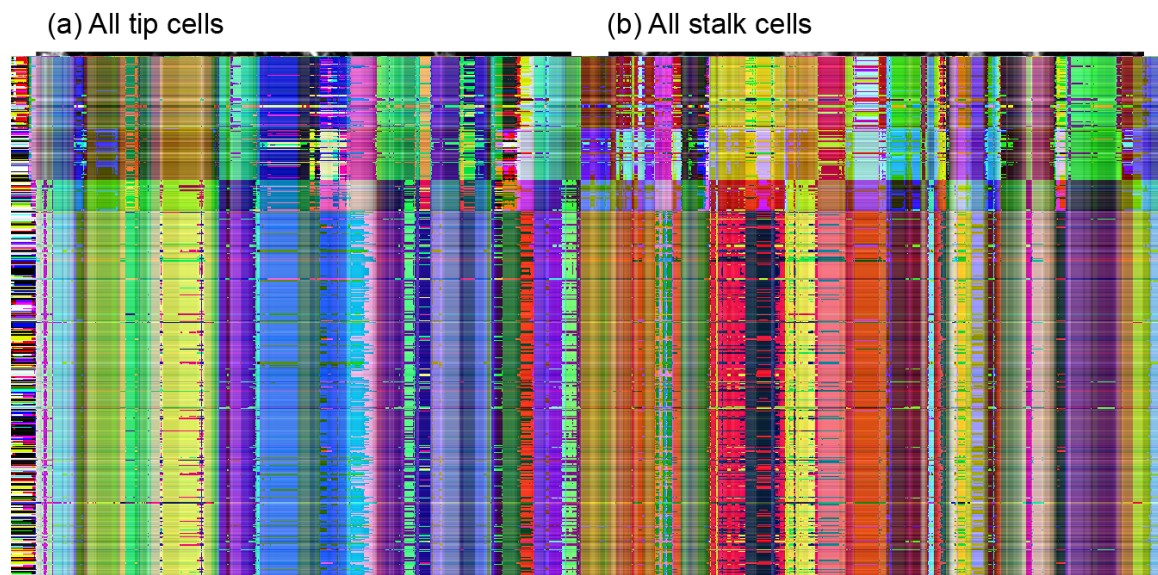
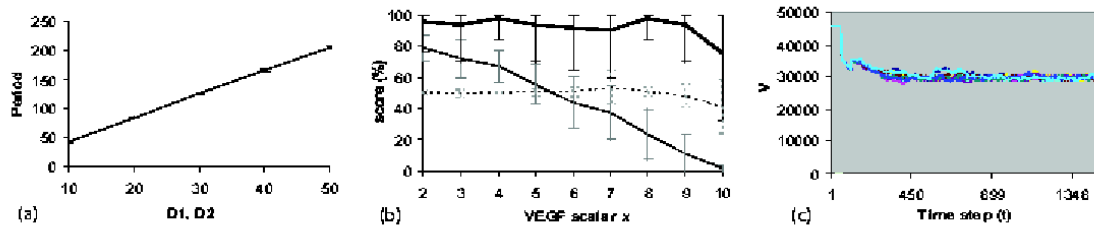


Fig 10



Accepted manuscript

Fig 11



Accepted manuscript